The Conformal Monogenic Signal⋆

Lennart Wietzke and Gerald Sommer

Kiel University, Institute of Computer Science, Chair of Cognitive Systems,
Christian-Albrechts-Platz 4, 24118 Kiel, Germany
{lw,gs}@ks.informatik.uni-kiel.de

Abstract. The *conformal monogenic signal* is a novel rotational invariant approach for analyzing i(ntrinsic)1D and i2D local features of two-dimensional signals (e.g. images) without the use of any heuristics. It contains the monogenic signal as a special case for i1D signals and combines scale-space, phase, orientation, energy and isophote curvature in one unified algebraic framework. The *conformal monogenic signal* will be theoretically illustrated and motivated in detail by the relation of the Radon and the Riesz transform. One of the main ideas is to lift up two-dimensional signals to a higher dimensional conformal space where the signal can be analyzed with more degrees of freedom. The most interesting result is that isophote curvature can be calculated in a purely algebraic framework without the need of any derivatives.

1 Introduction

In this paper 2D signals (e.g. gray value images) $f \in L_2(\Omega;\mathbb{R})$ with $\Omega \subset \mathbb{R}^2$ will be locally analyzed. Features such as phase ϕ, orientation θ and curvature κ will be determined at every test point $(x,y) \in \Omega$ of the original 2D signal f. For each test point a *local coordinate system* will be applied before analysis. One important local structural feature is the phase ϕ of a DC free 1D signal model $g(x) := a(x)\cos(\phi(x))$ which can be calculated by means of the Hilbert transform. Furthermore all signals will be analyzed in scale space (e.g. in Poisson scale space [1]) because the Hilbert transform can only be interpreted for narrow banded signals. One possible generalization of the Hilbert transform to higher dimensions which will be used in this work is the Riesz transform. 2D signals f are classified into local regions $N \subseteq \Omega$ of different intrinsic dimensions (also known as codimension):

$$f \in \begin{cases} \text{i0D}_N, f(\mathbf{x}_i) = f(\mathbf{x}_j) \, \forall \mathbf{x}_i, \mathbf{x}_j \in N \\ \text{i1D}_N, f(x,y) = g(x\cos\theta + y\sin\theta) \, \forall (x,y) \in N, f \notin \text{i0D}_N \\ \text{i2D}_N, \text{else} \end{cases} . \quad (1)$$

2   The Monogenic Signal

Phase and amplitude of 1D signals can be analyzed by the analytic signal. The generalization of the analytic signal to multidimensional signal domains has been done by the monogenic signal [2]. In case of 2D signals the monogenic signal delivers local phase, orientation and energy information. The monogenic signal can be interpreted for the application to i1D signals. This work presents the generalization of the monogenic signal for 2D signals to analyze both i1D and i2D signals in one single framework. The *conformal monogenic signal* delivers local phase, orientation, energy and curvature for i1D and i2D signals with the monogenic signal as a special case. To illustrate the motivation and the interpretation of this work, first of all the monogenic signal will be recalled in detail.

2.1   Riesz Transform

The monogenic signal replaces the Hilbert transform of the analytic signal by the Riesz transform which is known from Clifford analysis [3]. The Riesz transform $R\{\cdot\}$ extends the signal f to a monogenic (holomorphic) function. It is one possible, but not the only generalization of the Hilbert transform to multidimensional signal domains. In spatial domain the Riesz transform is given by the following convolution [4]:

$$R\{f\}(\mathbf{0}) := \frac{\Gamma(\frac{m+1}{2})}{\pi^{\frac{m+1}{2}}} \int\limits_{\mathbf{X}\in\mathbb{R}^m} \frac{f(\mathbf{x})}{\|\mathbf{x}\|^{m+1}}\mathbf{x}\,d\mathbf{x}\;. \tag{2}$$

In this work the Cauchy principal value (P.v.) of all integrals will be omitted. To enable interpretation of the Riesz transform, its relation to the Radon transform will be shown in detail. This relation can be proved by means of the Fourier slice theorem [5].

2.2   Relation of the Riesz and Radon Transform

The Riesz transform can be expressed using the Radon and the Hilbert transform. Note that the relation to the Radon transform is required solely for interpretation and theoretical results. Neither the Radon transform nor its inverse are ever applied to the signal in practice. Instead the Riesz transformed signal will be determined by convolution in spatial domain. The 2D Radon transform [6] is defined as:

$$r(t,\theta) := \mathcal{R}\{f\}(t,\theta) := \int\limits_{(x,y)\in\mathbb{R}^2} f(x,y)\delta_0(x\cos\theta + y\sin\theta - t)d(x,y) \tag{3}$$

with $\theta \in [0,\pi)$ as the orientation, $t \in \mathbb{R}$ as the minimal distance of the line to the origin $(0,0)$ and δ_0 as the Dirac delta distribution (see figure 1). The inverse
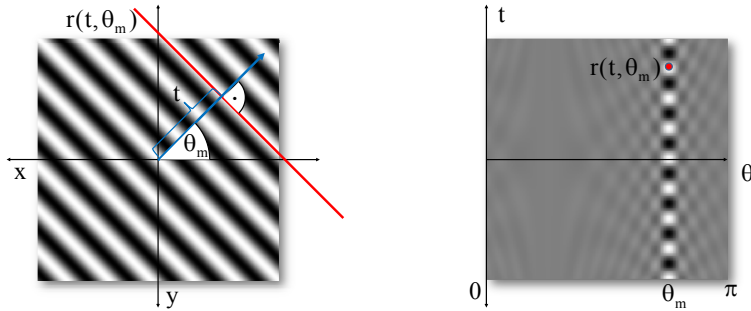
Fig. 1. Left figure: i1D signal f in spatial domain with orientation θ_m and local phase $\phi = 0$ at the origin $(0,0)$. Right figure: i1D signal f in Radon space. Each point in Radon space represents the integral in spatial domain on a line which is uniquely defined by the minimal distance $t \in \mathbb{R}$ to the origin and the orientation $\theta \in [0, \pi)$.

2D Radon transform exists and is defined by:

$$\mathcal{R}^{-1}\{r\}(x,y) := \frac{1}{2\pi^2} \int\limits_{\theta=0}^{\pi} \int\limits_{t \in \mathbb{R}} \frac{\frac{\partial}{\partial t} r(t, \theta)}{x \cos \theta + y \sin \theta - t} dt d\theta \ . \tag{4}$$

Now the Riesz transform will be expressed by the Hilbert transform, the Radon transform and its inverse:

$$R\{f\}(x,y) = \mathcal{R}^{-1}\left\{ \begin{bmatrix} \cos \theta \\ \sin \theta \end{bmatrix} h_1(t) * r(t, \theta) \right\}(x,y) \tag{5}$$

with $h_1(t) = \frac{1}{\pi t}$ as the one-dimensional Hilbert kernel and $*$ as the convolution operator. In other words the Riesz transform applies a one-dimensional Hilbert transform to the Radon space representation $r(t, \theta)$ of the signal along $t \in \mathbb{R}$ for each orientation $\theta \in [0, \pi)$ separately. For the following implications the signal is defined by a superposition of i1D signals $f := \sum_{i \in I} f_i$ where each i1D signal f_i is orientated along θ_i. To be able to extract orientation and phase information from the Riesz transformed signal, the inverse Radon transform must be simplified. This can be achieved by two assumptions. Firstly, the point of interest where local feature information should be obtained will be translated to the origin $(0,0)$ for each point $(x,y) \in \Omega \subset \mathbb{R}^2$ so that the inverse 2D Radon transform has to be evaluated only at $(x,y) := (0,0)$.

Let be $M := [0, \pi) - \bigcup_{i \in I}\{\theta_i\}$ the set of all orientations where no i1D signal information exists. Secondly, the θ-integral of the inverse Radon transform vanishes because $r(t_1, \theta) = r(t_2, \theta) \ \forall t_1, t_2 \in \mathbb{R} \ \forall \theta \in M$ implies $\frac{\partial}{\partial t} r(t, \theta) = 0 \ \forall t \in \mathbb{R} \ \forall \theta \in M$ for a finite number $\|I\| \in \mathbb{N}$ of superimposed i1D signals. Because of this fact (and the linearity property of the Radon transform), the θ-integral of the inverse Radon transform can be replaced by a finite sum of discrete angles θ_i to enable modeling the superposition of an arbitrary number of i1D signals.

Therefore the inverse Radon transform can be written as:

$$\mathcal{R}^{-1}\{r\}(0,0) = -\frac{1}{2\pi^2} \sum_{i \in I} \int_{t \in \mathbb{R}} \frac{\frac{\partial}{\partial t} r(t, \theta_i)}{t} dt . \tag{6}$$

Now the 2D Riesz transform and therefore the monogenic signal can be interpreted in an explicit way.

2.3 Interpretation of the 2D Riesz Transform

Because of the property $\frac{\partial}{\partial t}(h_1(t) * r(t, \theta)) = h_1(t) * \frac{\partial}{\partial t} r(t, \theta)$ the 2D Riesz transform of any i1D signal with orientation θ_m results in:

$$\begin{bmatrix} R_x\{f\}(0,0) \\ R_y\{f\}(0,0) \end{bmatrix} = \underbrace{-\frac{1}{2\pi^2} \int_{t \in \mathbb{R}} \frac{1}{t} h_1(t) * \frac{\partial}{\partial t} r(t, \theta_m) dt}_{=:s(\theta_m)} \begin{bmatrix} \cos\theta_m \\ \sin\theta_m \end{bmatrix} . \tag{7}$$

The orientation of the signal can therefore be derived by:

$$\theta_m = \arctan\frac{s(\theta_m)\sin\theta_m}{s(\theta_m)\cos\theta_m} = \arctan\frac{R_y\{f\}(0,0)}{R_x\{f\}(0,0)} . \tag{8}$$

The partial Hilbert transform [7] of $f_{\theta_m}(\tau) := f(\tau\cos\theta_m, \tau\sin\theta_m)$ and therefore also its phase can be calculated by:

$$\phi = \operatorname{atan2}\left((h_1 * f_{\theta_m})(0), f(0,0)\right) \tag{9}$$

$$= \operatorname{atan2}\left(\sqrt{R_x^2\{f\}(0,0) + R_y^2\{f\}(0,0)}, f(0,0)\right) . \tag{10}$$

This reveals that - although the Riesz transform is a generalization of the Hilbert transform to multi-dimensional signal domains - it still applies a one-dimensional Hilbert transform along the main orientation θ_m to the signal. In short, the monogenic signal enables interpretation of i1D signals and the mean value of their superposition [8].

3 The Conformal Monogenic Signal

The feature space of the 2D monogenic signal is spanned by phase, orientation and energy information. This restriction correlates to the dimension of the associated Radon space. Therefore, the feature space of the 2D signal can only be extended by lifting up the original signal to higher dimensions. This is one of the main ideas of the *conformal monogenic signal*. In the following the 2D monogenic signal will be generalized to analyze also i2D signals by embedding the 2D signal into the conformal space. The previous section shows that the 2D Riesz transform can be expressed by the 2D Radon transform which integrates all function values on lines. This restriction to lines is one of the reasons why
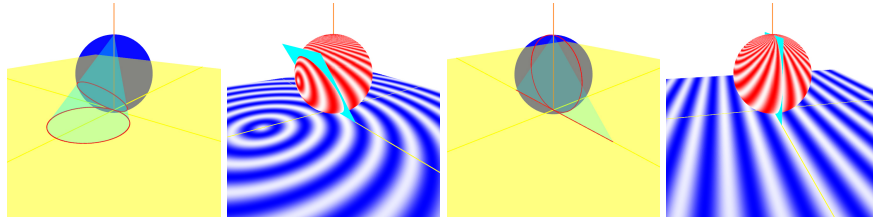
Fig. 2. Circles on the original 2D plane are mapped to circles on the sphere passing not the north pole $(0, 0, 1)$. Lines on the plane are mapped to circles passing through the north pole, i.e. lines are a special case of circles with infinite radius.

the 2D monogenic signal is limited to i1D signals (such as lines and edges) with zero isophote curvature. To analyze also i2D signals and to measure curvature $\kappa = \frac{1}{\rho}$, a 2D Radon transform which integrates on curved lines (i.e. circles with radius ρ) is preferable. Unfortunately, the inverse Radon transform directly on circles is not unique [9]. Now it will be proposed to solve this problem in conformal space. In 3D signal domains the Radon transform integrates on planes, although at first sight 3D planes are not related to 2D signals. The idea is that circles form the intersection of a sphere (with center at $\left(0, 0, \frac{1}{2}\right)$ and radius $\frac{1}{2}$) and planes passing through the origin $(0, 0, 0)$. Since the Riesz transform can be extended to any dimension and the 3D Riesz transform can be expressed by the 3D Radon transform, the 2D signal coordinates must be mapped appropriately to the sphere. This mapping must be conformal (i.e. angle preserving), so that interpretation of the 3D Riesz transform in conformal space is still reasonable. Analogous to the (t, θ) line parametrization of the 2D Radon transform, the planes of the 3D Radon transform are uniquely defined by the parameters (t, θ, φ). This new parametrization (see figure 4) truly extends the interpretation space of the monogenic signal by one dimension. Now the 2D signal will be embedded into a two-dimensional subspace of the conformal space.

3.1 The Conformal Space

The main idea is that the concept of lines in 2D Radon space becomes the more abstract concept of planes in 3D Radon space. These planes determine circles on the sphere in conformal space. Since lines and circles of the two-dimensional signal domain are mapped to circles [10] on the sphere (see figure 2), the integration on these circles determines points in the 3D Radon space. The stereographic projection $\mathcal{C}$ known from complex analysis [11] maps the 2D signal domain to the sphere (see figure 3). This projection is conformal and can be inverted by $\mathcal{C}^{-1}$ for all elements of $S \subset \mathbb{R}^3$:

$$S := \left\{ (x, y, z) \in \left[-\frac{1}{2}, \frac{1}{2}\right]^2 \times [0, 1) : x^2 + y^2 + (z - \frac{1}{2})^2 = \frac{1}{4} \right\} \qquad (11)$$

$$S^{\mathbb{R}^2} \ni \mathcal{C}(x,y) := \frac{1}{x^2 + y^2 + 1} \begin{bmatrix} x \\ y \\ x^2 + y^2 \end{bmatrix}, \quad \mathcal{C}^{-1}(x,y,z) := \frac{1}{1-z} \begin{bmatrix} x \\ y \end{bmatrix}. \quad (12)$$

This mapping has the property that the origin $(0,0)$ of the 2D signal domain will be mapped to the south pole $\mathbf{0} := (0,0,0)$ of the sphere and both $-\infty, +\infty$ will be mapped to the north pole $(0,0,1)$ of the sphere. Lines and circles of the 2D signal domain will be mapped to circles on the sphere and can be determined uniquely by planes in 3D Radon space. The integration on these planes corresponds to points (t,θ,φ) in the 3D Radon space.
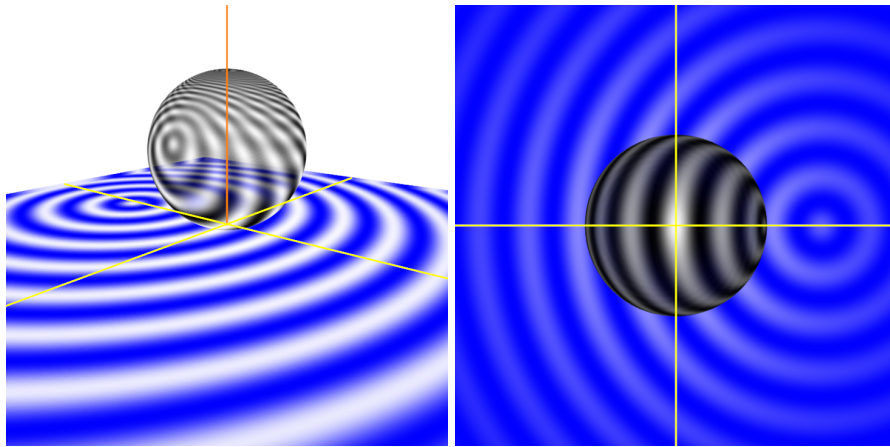

Fig. 3. Left and right figure show the conformal space from two different point of views. The 2D signal f will be mapped by the stereographic projection on the sphere.

3.2 The Riesz Transform in Conformal Space

Since the signal domain $\Omega \subset \mathbb{R}^2$ is bounded, not the whole sphere is covered by the original signal (see left part of figure 4). Anyway, all planes corresponding to circles remain unchanged. That is the reason why the *conformal monogenic signal* models i1D lines and all kinds of curved i2D signals which can be locally approximated by circles. To give the Riesz transform more degrees of freedom, the original two-dimensional signal will be embedded in a applicable subspace of the conformal space by:

$$\mathbb{R}^{\mathbb{R}^3} \ni c(x,y,z) := \begin{cases} f(\mathcal{C}^{-1}(x,y,z)^T) & , x^2 + y^2 + \left(z - \frac{1}{2}\right)^2 = \frac{1}{4} \\ 0 & , \text{else} \end{cases}. \quad (13)$$

Thus, the 3D Riesz transform can be applied to all points on the sphere. The center of convolution in spatial domain is the south pole $(0,0,0)$ where the origin
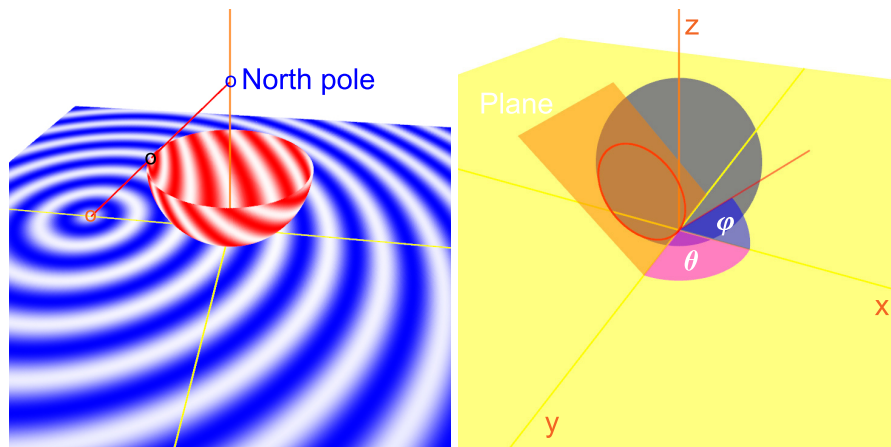
Fig. 4. Left figure: The stereographic projection ray passes through each 2D point (x, y) and the north pole $(0, 0, 1)$ of the sphere. The conformal mapping of the point (x, y) is defined by the intersection of its projection ray and the sphere. Right figure: Each intersection of the sphere and a plane passing through the origin $(0, 0, 0)$ delivers a circle. Those planes and thus all circles on the sphere are uniquely defined by the angles (θ, φ) of the normal vector.

of the 2D signal domain meets the sphere. At this point the 3D Riesz transform will be performed. Now the *conformal monogenic signal* can be introduced by the 3D Radon transform and its inverse analogous to the monogenic signal in 2D:

$$
\begin{bmatrix} c(\mathbf{0}) \\ R_x\{c\}(\mathbf{0}) \\ R_y\{c\}(\mathbf{0}) \\ R_z\{c\}(\mathbf{0}) \end{bmatrix} := \begin{bmatrix} c(0,0,0) \\ \mathcal{R}^{-1}\left\{ \begin{bmatrix} \sin\varphi\cos\theta \\ \sin\varphi\sin\theta \\ \cos\varphi \end{bmatrix} h_1(t) * \mathcal{R}\{c\}(t,\theta,\varphi) \right\}(0,0,0) \end{bmatrix} \quad (14)
$$

and without loss of generality the signal will be analyzed at the origin $\mathbf{0} = (0, 0, 0)$. Compared to the 2D monogenic signal the *conformal monogenic signal* performs a 3D Riesz transformation in conformal space.

3.3 The Radon Transform in Conformal Space

To interpret the *conformal monogenic signal*, the relation to the 3D Radon transform in conformal space must be taken into account. The 3D Radon transform is defined as the integral of all function values on the plane defined by $(t, \theta, \varphi) \in \mathbb{R} \times [0, 2\pi) \times [0, \pi)$:

$$
\mathcal{R}\{c\}(t, \theta, \varphi) = \int_{\mathbf{x} \in \mathbb{R}^3} c(\mathbf{x})\delta_0(\mathbf{x} \begin{bmatrix} \sin\varphi\cos\theta \\ \sin\varphi\sin\theta \\ \cos\varphi \end{bmatrix} - t)d\mathbf{x} . \quad (15)
$$

Since the signal is mapped on the sphere and all other points of the conformal space are set to zero, the 3D Radon transform actually sums up all points lying on the intersection of the plane and the sphere. For all planes this intersection can be either empty or a circle. The concept of circles in the conformal 3D Radon transform can be compared with the concept of lines known from the 2D Radon transform. Since lines in the 2D domain are also mapped to circles, the *conformal monogenic signal* can analyze i1D as well as curved i2D signals in one single framework. The inverse 3D Radon transform exists and differs from the 2D case such that it is a *local* transformation [12]. That means the Riesz transform at $(0,0,0)$ is completely determined by all planes passing the origin (i.e. $t = 0$). In contrast, the 2D monogenic signal requires all integrals on all lines (t, θ) to reconstruct the original signal at a certain point and is therefore called a *global* transform. This interesting fact turns out from the following 3D inverse Radon transform:

$$\mathcal{R}^{-1}\{r\}(\mathbf{0}) := -\frac{1}{8\pi^2} \int\limits_{\theta=0}^{2\pi} \int\limits_{\varphi=0}^{\pi} \frac{\partial^2}{\partial t^2} \, r(t, \theta, \varphi)|_{t=0} \, d\varphi d\theta \ . \tag{16}$$

Therefore, the local features of i1D and i2D signals can be determined by the *conformal monogenic signal* at the origin of the 2D signal without knowledge of the whole Radon space. Hence, the relation of the Radon and the Riesz transform is essential to interpret the Riesz transform in conformal space.

3.4 Interpretation and Experimental Results

Analogous to the interpretation of the monogenic signal, the parameters of the plane within the 3D Radon space determine the local features of the curved i2D signal. The *conformal monogenic signal* can be called the generalized monogenic signal for i1D and i2D signals, because lines and edges can be considered as circles with zero curvature. These lines are mapped to circles passing through the north pole in conformal space. The curvature can be measured by the parameter φ of the 3D Radon space:

$$\varphi = \arctan \frac{R_z\{c\}(\mathbf{0})}{\sqrt{R_x^2\{c\}(\mathbf{0}) + R_y^2\{c\}(\mathbf{0})}} \ . \tag{17}$$

It can be shown that φ corresponds to the isophote curvature κ known from differential geometry [13, 14]:

$$\kappa = \frac{-f_{xx}f_y^2 + 2f_x f_y f_{xy} - f_{yy}f_x^2}{\left(f_x^2 + f_y^2\right)^{\frac{3}{2}}} \ . \tag{18}$$

Besides, the curvature of the *conformal monogenic signal* naturally indicates the intrinsic dimension of the signal. The parameter θ will be interpreted as the orientation in i1D case and deploys to direction $\theta \in [0, 2\pi)$ for the i2D case:

$$\theta = \operatorname{atan2}\left(R_y\{c\}(\mathbf{0}), R_x\{c\}(\mathbf{0})\right) \ . \tag{19}$$

The phase is defined by ϕ for all intrinsic dimensions by

$$\phi = \text{atan2} \left(\sqrt{R_x^2 \left\{ c \right\} (\mathbf{0}) + R_y^2 \left\{ c \right\} (\mathbf{0}) + R_z^2 \left\{ c \right\} (\mathbf{0})}, c(\mathbf{0}) \right) \ . \qquad (20)$$

All proofs are analogous to those shown for the 2D monogenic signal. The *conformal monogenic signal* can be efficiently implemented by convolution in spatial domain without the need of any Fourier transform. Since the 3D convolution in conformal space can be simplified to a faster 2D convolution on the sphere, the time complexity of the *conformal monogenic signal* computation is in $O(n^2)$ with n as the convolution mask size in one dimension. On synthetic signals the error of the feature extraction converges to zero with increasing refinement of the convolution mask. The advantages of the monogenic isophote curvature compared to the curvature delivered by the classical differential geometry [15] approach can be seen clearly in figure 5. Under the presence of noise the monogenic isophote curvature performs in general more robust than the classical isophote curvature. Detailed application and performance behavior of the *conformal monogenic signal* will be part of future work.
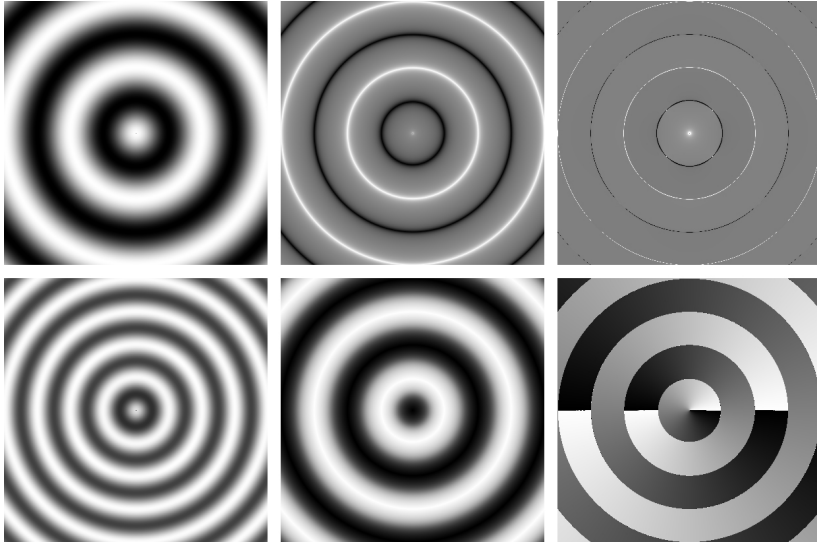

Fig. 5. Experimental results and comparison. Top row from left to right: Synthetic signal, monogenic isophote curvature and classical isophote curvature determined by derivatives. Bottom row from left to right: Energy, phase and direction. Convolution mask size: 5×5 pixels.

4 Conclusion

In this paper a novel generalization of the monogenic signal for two-dimensional signals has been presented to analyze i(ntrinsic)1D and i2D signals in one unified algebraic framework. The idea of the *conformal monogenic signal* is to lift up two-dimensional signals to an appropriate conformal space in which the signal can be Riesz transformed with more degrees of freedom compared to the 2D monogenic signal. Without steering i1D and i2D local features such as phase, orientation/direction, energy and isophote curvature can be determined in spatial domain. The *conformal monogenic signal* can be computed efficiently with same time complexity as the 2D monogenic signal. Furthermore, the exact local isophote curvature (which is of practical importance in low level image analysis) can be calculated without the need of derivatives. Hence, all problems of partial derivatives on discrete grids can be avoided by the application of the *conformal monogenic signal*.

References

1. Felsberg, M., Sommer, G.: The monogenic scale-space: A unifying approach to phase-based image processing in scale-space. Journal of Mathematical Imaging and Vision (2003)
2. Felsberg, M., Sommer, G.: The monogenic signal. Technical report, Kiel University (2001)
3. Brackx, F., De Knock, B., De Schepper, H.: Generalized multidimensional hilbert transforms in clifford analysis. International Journal of Mathematics and Mathematical Sciences (2006)
4. Delanghe, R.: Clifford analysis: History and perspective. In: Computational Methods and Function Theory. Volume 1. (2001) 107–153
5. Stein, E.M.: Singular Integrals and Differentiability Properties of Functions. Princeton University Press (1971)
6. Beyerer, J., Leon, F.P.: The radon transform in digital image processing. Automatisierungstechnik **50**(10) (2002) 472–480
7. Hahn, S.L.: Hilbert Transforms in Signal Processing. Artech House (1996)
8. Wietzke, L., Sommer, G., Schmaltz, C., Weickert, J.: Differential geometry of monogenic signal representations. In: Robot Vision, Springer (2008) 454–465
9. Ambartsoumian, G., Kuchment, P.: On the injectivity of the circular radon transform. In: Inverse Problems. Volume 21., Inst. of Physics Publishing (2005) 473
10. Needham, T.: Visual Complex Analysis. Oxford University Press (1997)
11. Gürlebeck, K., Habetha, K., Sprössig, W.: Funktionentheorie in der Ebene und im Raum (Grundstudium Mathematik). Birkhäuser Basel (2006)
12. Bernstein, S.: Inverse probleme. Technical report, TU Bergakdemie Freiberg (2007)
13. do Carmo, M.P.: Differential Geometry of Curves and Surfaces. Prentice-Hall (1976)
14. Baer, C.: Elementare Differentialgeometrie. Volume 1. de Gruyter, Berlin, New York (2001)
15. Lichtenauer, J., Hendriks, E.A., Reinders, M.J.T.: Isophote properties as features for object detection. In: CVPR (2), IEEE Computer Society (2005) 649–654